Cell. Mol. Biol. 58 (1): 44-49
Published on December 22, 2012
DOI 10.1170/T919

Cellular & Molecular Biology
http://www.cellmolbiol.com

CHARACTERIZATION OF CATALYTIC CARBOXYLATE TRIAD IN NON-REPLICATIVE DNA POLYMERASE III (pol E) OF *Geobacillus kaustophilus* HTA

C. SANDALLI[1], K. SINGH[2,3] AND M. J. MODAK [3] ✉

[1] Department of Biology, Faculty of Arts & Sciences, Recep Tayyip Erdoğan University, 53100 Rize, Turkey

[2] Christopher Bond Life Sciences Center, University of Missouri, Columbia, MO 65211, USA

[3] Department of Biochemistry and Molecular Biology, UMDNJ-New Jersey Medical School, Newark, NJ, USA

Abstract

Three aspartic acid residues D378, D380 and D531 form the catalytic carboxylate triad in *Geobacillus kaustophilus (Gka)* DNA polymerase III α-subunit homolog, pol E. We cloned, expressed and purified wild type (WT), alanine (D → A) and glutamate (D → E) mutant enzymes of D378, D380 and D531. The WT and mutant enzymes were biochemically characterized for DNA binding, dNTP binding and catalytic activity in the presence of two metal ions (Mg^{2+} and Mn^{2+}). The polymerase activity of all mutant enzymes was lost in the presence Mg^{2+}, whereas D378E and D531E mutant enzymes showed about 35 and 60 percent activity, with Mn^{2+}. D380E mutant enzyme did not show noticeable activity with either metal ions suggesting its absolute requirement in polymerase reaction. Kinetic characterization of individual mutant proteins showed that the template-primer binding affinity ($K_{D.DNA}$) did not change due to both D → A or D → E mutation. The $K_{M.dNTP}$ for D378E and D531E increased by about 10- and 100-fold, compared to WT enzyme implicating the function of these residues in dNTP binding. Based on these results and the analysis of the available crystal structures of the homologous enzyme species in their apo and E.DNA.dNTP ternary complex forms, we conclude that D378 and D531 are mainly responsible for the binding of metal chelated substrate dNTP, while D380 is solely responsible for the chemical step of phosphodiester bond formation.

Key words: *Geobacillus kaustophilus* HTA, DNA polymerase III, DNA pol E active site asparates , divalent cation effects, DNA binding, dNTP binding.

Article information

Received on May 14, 2012
Accepted on September 13, 2012

✉ **Corresponding author**
Tel: +973-972-5515
Fax: +973-972-5594
E-mail:modak@umdnj.edu

INTRODUCTION

DNA polymerases are integral part of genome maintenance and replication in both eukaryotic and prokaryotic systems of life. Early sequence alignments revealed the presence of conserved blocks of amino acid residues (motifs A to F) present in DNA polymerases from different species (6,14,15). The conserved acidic amino acid residues (aspartate/glutamate) in motifs A and C were postulated to serve as metal ligands for divalent cations during phosphoryl transfer reaction catalyzed by replication enzymes. The extensive structural studies have shown that DNA polymerases from wide variety of sources exhibit a common architectural layout that resembles the half-open right hand (21,31,34). Therefore, various structural units have been termed as the fingers, thumb and palm subdomains (21,35). The palm subdomain is highly conserved among DNA polymerases, as it constitutes the catalytic core. The palm also contains catalytic carboxylates from motifs A and C. These carboxylates participate in the catalytic process by providing the binding sites for the two divalent metal ions that are liganded to the phosphate moieties of dNTP (8,13,22,24). One of the two metals (referred to as metal A) has been proposed to function in the chemistry of phosphodiester bond formation while the other metal (metal B) has been suggested to serve as structural metal which stabilizes the triphosphate moiety of dNTP prior to bond formation and neutralizes the charge of leaving pyrophosphate moiety after the bond formation (10,35, 36). The fingers and the thumb subdomains exhibit wide variation, both at the secondary and tertiary structure levels (7,16,23). Using pre-state-state kinetics, minimal general reaction mechanism of DNA polymerase has been established (17), and most DNA polymerases utilize steps of this reaction scheme. According this reaction mechanism, a typical DNA polymerase first binds template-primer to form E.DNA binary complex. The dNTP binding occurs to this complex to form an 'open' E.DNA.dNTP ternary complex. A rigid body movement of fingers subdomain brings the dNTP in a 'closed' catalytically competent conformation poised for catalysis. The dNTP substrate at this state is held in-place through the interaction between catalytic carboxylates and triphosphate moiety of dNTP mediated by divalent cations. The divalent cations not only align the dNTP for catalysis, they also coordinate with 3'OH moiety of primer and generate a nucleophile. Highly structured tetragonal bi-pyramid geometry has been proposed as a result from the metal coordination (33,34). The DNA polymerases can use either Mg^{2+} or Mn^{2+} as divalent cations. Both cations can form octahedral bi-pyramid coordination geometry; however, the differences in coordination of the two metal ions at the active site of DNA polymerases (if any) are not known.

As discussed above, the carboxylate residues are critical constituents of the catalytic center of DNA polymerases and have consequently become the landmark feature of DNA polymerase active site. While most DNA polymerases contain three carboxylates, some variation in the absolute requirement of only two of the three or all three carboxylates in the catalytic process has persisted. For example, in *E. coli* DNA polymerase I, only two aspartates (D705 and D882) are required for catalysis (18,25,26). However, in α-subunits *E. coli* DNA pol III, and in retroviral reverse transcriptases, all three carboxylates are required for activity (20,27). In order to clarify the absolute requirement of two or three carboxylates in pol III and related enzymes

and to understand the role of individual asprtates in these enzymes, we made alanine and glutamate substitutions at the three individual aspartates in DNA pol III homolog, pol E from *Geobacillus kaustophillus* HTA *(Gka)* and investigated their effects on the polymerase activity. We find that the alanine substitution at any one of the three carboxylate renders the enzyme inactive. However, the homologous mutation of aspartate to glutamate at two of the three sites is well tolerated, particularly in presence of Mn^{2+} as a divalent cation. Based on these results and other structural characteristics of the apo and ternary complex structures of pol III, we conclude that two aspartates are required for the substrate dNTP binding, while the third one is required for the step of bond formation.

MATERIALS AND METHODS

Materials

The PCR grade dNTPs were from Roche Applied Science. Radiolabeled nucleotides were obtained from PerkinElmer Life Sciences. The DNA extraction kit was from Qiagen, whereas DNA oligodeoxynucleotides were either from MWG-Biotechnologies or from the Molecular Resources Facility at the New Jersey Medical School, Newark, NJ. All ^{32}P-5′-end-labeled oligomers were purified by denaturing polyacrylamide-urea gel electrophoresis as described previously (1,12,32).

Cloning, expression and purification of WT Gka polIII (pol E)

Geobacillus kaustophilus HTA (*Gka*) was obtained from the glycerol stock deposited in the Karadenzi Technical University, Molecular Biology Laboratory (Trabzon, TURKEY). The bacterium was grown in Luria-Bartani (LB) medium at 55 °C and the genomic DNA was purified using Wizard Genomic DNA Purification Kit (Promega, Madison, USA). *Gka* DNA E gene was amplified by two specific primers (GkaFw: 5'-ATAGGATCCGATGATGTTCGTCCACTTGC-3'and GkaRv: 5'– ATAGGATCCTTACTTGACGAC-CACGCGTCC–3'). Both primers contain *Bam*HI restriction site (underlined) to allow in-frame ligation into the pET-28a expression vector (Novagene). The gene amplification by PCR was performed using 2.5 units of Expand High Fidelity *Taq* DNA polymerase (Fermentas) in a 50 µl reaction mixture containing 0.2 mM of dNTP mixture, 300 ng of each primer, and 100 ng of genomic DNA. A predicted 3.76 kb DNA fragment obtained from PCR, was digested with *Bam*HI and ligated into the pET-28a expression vector. The resulting recombinant plasmid was transformed into *E. coli* BL21 (DE3) pLysS for overexpression. The expression was carried out as detailed by Sandalli et al. (28). The recombinant enzyme containing N-terminal hexa-histidine-tag was purified by nickel-affinity column using a protocol suggested by manufacturer (Promega). were grown to an optical density at 600 nm of about 0.6 in LB medium containing 50 µg/ml ampicillin at 37°C, and expression was induced by the addition of 1 mM isopropyl β-D-thiogalactopyranoside. After induction for 3 h at 37°C, the cells were harvested by centrifugation. The recombinant *Gka* pol E and its mutant derivatives were purified by performing heat treatment and nickel affinity chromotography (28).

Site-directed mutagenesis of catalytic carboxylates (D378A, D378E, D380A, D380E, D531A, D531E and D3783E/D531E)

We used a PCR based protocol as described in Stratagene's QuickChange site-directed mutagenesis kit to generate the desired mutations in DNA *pol E*. The pET28a plasmid containing the *Gka* pol III gene was used for generating mutant derivatives, and all mutations were confirmed by DNA sequencing of plasmid. The mutant enzymes were purified using the protocol standardized for WT enzyme.

Determination of DNA binding affinity ($K_{D.DNA}$)

We used gel mobility shift assay to determine the the binding affinity of template-primer to the WT and mutant *Gka* pol E enzymes. To determine the binding affinity of template-primer to the desired enzymes, gel mobility shift assays were performed as described previously (12). The binding of 1 nM 63/14-mer template-primer (sequence is shown in fig 1) to various concentrations of enzyme (5 to 100 nM) was carried out in a reaction mixture containing 50 mMTris-HCl, pH 7.8, 5 mM $MgCl_2$, 10% (v/v) glycerol, and 0.1 mg/ml bovine serum albumin. Different protein concentrations were used to bracket the $K_{D.DNA}$ value. Samples were electrophoresed at 100 V for 1.5 h at 4°C on a 6% nondenaturing polyacrylamide gel, using 89 mM Tris borate, pH 8.2, buffer. Gel were dried, then scanned in a PhosphorImager and quantitated by ImageQuant software (Amersham Biosciences). The percent enzyme-TP binding was calculated by quantifying the amount of uncomplexed TP in each lane. Percent binding values were then used for the determination of $K_{D.DNA}$ by interpolation, using nonlinear regression for one-site binding (hyperbola) with GraphPad Prism software.

Determination of steady-state kinetic constants (kcat and $K_{M.dNTP}$)

Determination of $K_{M.dNTP}$ single nucleotide incorporation by *Gka* polIII (pol E) was carried out at 55 °C. Five dATP concentrations ranging between 0 to 20 µM were used to determine $K_{m.dNTP}$. The reaction mixtures (6 µl) containing 5 mM $MgCl_2$ or 2 mM $MnCl_2$, 2 nM 5-end-^{32}P-labeled 63/14-mer template-primer (the next incoming dNTP is dATP) and 10 nM *Gka* pol E were incubated with varying concentrations of dNTP. The reactions were stopped at 30 sec by 6 µl Sanger's gel loading dye (29). The extended primers were resolved on 16% acrylamide-8M urea gel followed by visualization and quantitation as described above. The data were processed as described by Astatke et al (2).

RESULTS AND DISCUSSION

Comparative analyses of the primary amino acid sequences of many DNA polymerases revealed that certain blocks of sequences (called motifs A to F) are highly conserved. One aspartate in motif A and motif C is present in all DNA polymerases. However, in some DNA polymerases such as mammalian DNA polymerase β (30) and prokaryotic pol C (3,9) a second aspartate is also present in motif A. In other DNA polymerases such as *E.coli* pol I and HIV-1 RT, second carboxylate is present in motif C. One carboxylates from each motif has been shown to be critical for polymerase activity (31,11). A detailed analy-

sis of 4 carboxylates, inferred from the results of the properties of the alanine mutant species of these enzymes, showed that only two aspartates were absolutely essential, while the 3rd and 4th ones provided strong activity enhancing effects (11). In fact, Steitz has proposed a mechanistic model for the binding of two divalent metal ions, called metal A (catalytic metal) and metal B (structural metal), to two aspartates and phosphate oxygens of incoming dNTP, forming a tetragonal bipyramide (octahedral) geometry, which represents an active state intermediate in the polymerase reaction (35). A recent pre-steady state analysis of the pre-polymerase complex formation in KF of *E. coli* DNA polymerase, using alanine mutant of two essential carboxylates has further confirmed that one aspartate (D705) is involved in ternary complex formation, while the other (D882) provides a site for the binding of metal A, which in turn activates the catalytic complex (4). In view of this scenario, it was not clear, how the polymerases requiring participation of 3 aspartates, such as retroviral reverse transcriptases as well as prokaryotic pol III (5,27,19) functioned.

The present study, using *Geobacillus kaustophilus* pol E, a pol III homolog, as a representative of polymerases that utilize 3 aspartates at the active center, was undertaken to clarify the role of individual aspartate. The identity of these aspartates was predicted from primary amino acids sequence comparison of few related polymerases and from the two crystal structures of the related homologues enzymes (3,9). We first confirmed that all three aspartates are required for the catalytic activity (Table 1) as their individual mutation to alanine exhibited near complete loss of activity. This loss of activity remained unchanged, when Mg^{2+} was replaced by Mn^{2+} in the reaction mixture (Figure 1A and B).

When aspartic acid was replaced with glutamic acid, maintaining the same negative charge but the length of the acidic side chain is reduced by one C-C bond (methylene unit), a somewhat different activity pattern was noted, only with Mn^{2+} containing reaction mixtures. In this case, some recovery of polymerase activity was clearly seen with two of the three mutant enzymes. The two active mutant enzymes were D378E and D531E, while the mutant enzyme D380E remained inactive. In order to further clarify the contribution of two partially active glutamate mutant

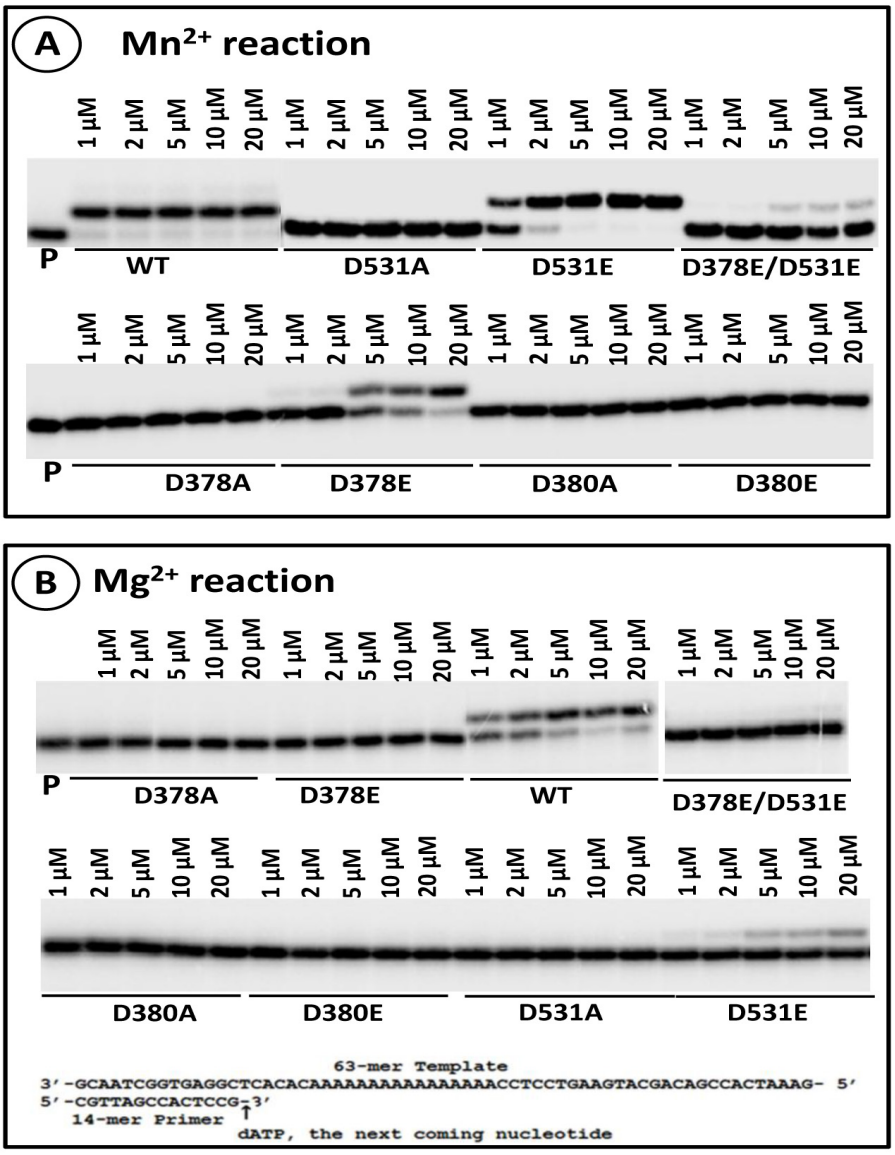

Figure 1. Polymerase activity of WT and active site aspartates mutants in presence of Mg^{2+} or Mn^{2+}: This figure shows the incorporation of a single nucleotide by WT and active site aspartate mutant derivatives of *Gka* pol E in the presence of either 1 mM $MnCl_2$ (panel A) or 5 mM $MgCl_2$ (panel B). The reactions were carried out at 55 °C for 30 minutes with increasing concentration of dATP (0 to 20 µM). The $K_{M.dNTP}$ was determined by plotting the initial velocity against dNTP concentration. The template-primer sequence is given in panel B.

Table 1. Kinetic parameters of WT and active site mutant *Gka* pol E enzymes.

Enzyme	$K_{D.DNA}$ (nM)	Activity (Mg^{2+}) (% WT)	$K_{m.dNTP}$ (μM) (Mg^{2+})[a]	Activity (Mn^{2+}) (%WT)	$K_{m.dNTP}$ (μM) (Mn^{2+})
WT	24.0 ± 1.2	100	0.14 ± 0.01	100	1.5 ± 0.2
D378A	27.4 ± 4.8	<0.5	No Activity	<0.5	No Activity
D378E	33.8 ± 1.3	<1.0	18.50 ± 1.6	34.0	No Activity
D380A	24.9 ± 2.7	<0.5	No Activity	<0.5	No Activity
D380E	21.5 ± 4.0	<0.5	No Activity	<0.5	No Activity
D531A	50.8 ± 6.8	<1.0	No Activity	<0.5	No Activity
D531E	14.4 ± 1.0	<1.0	1.3 ± 0.8	58.0	17.24 ± 1.4
D378E/D531E	52.4 ± 4.8	<1.0	No Activity	3.0	No Activity

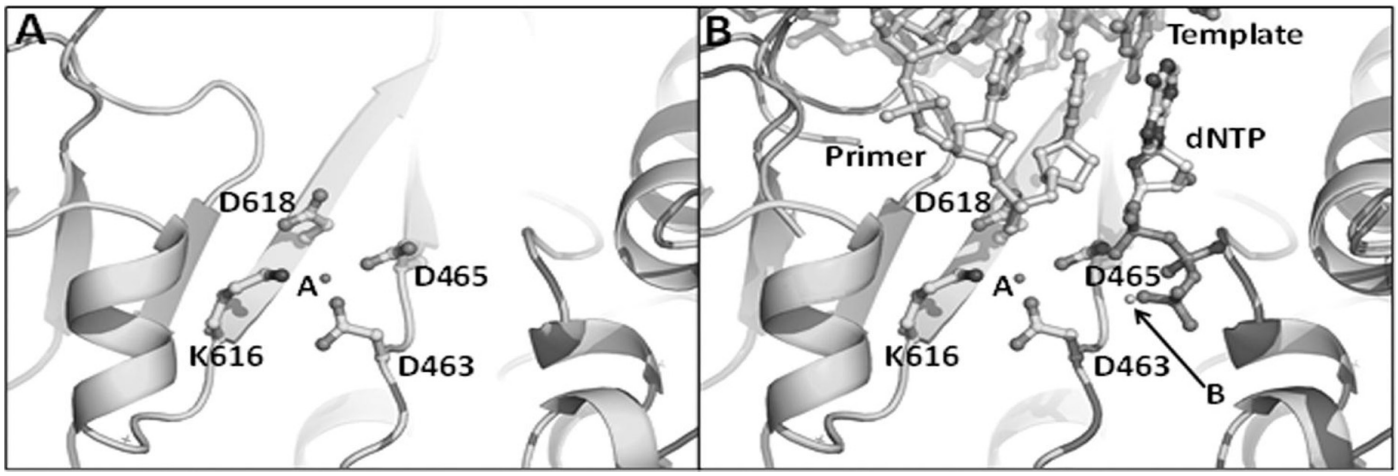

Figure 2. Position of metal ions at the active site of pol III: Panel A shows the close-up view of active site of *T.aquaticus* pol III and panel B shows the superposition of apo and ternary complex of the same enzyme. Metal ions A and B are shown as dots. The catalytic aspartates and a conserved lysine are rendered in ball-and-stick mode.

enzymes, a double mutant enzyme (D378E/D531E) was generated and tested for polymerase activity. Interestingly, the simultaneous mutation of both aspartates (D378 and D531) to glutamate had less than 3% activity in Mn^{2+} catalyzed reaction and no activity with Mg^{2+} catalyzed reactions (Fig. 1 and Table 1). These observations suggest that homologous substitution of glutamate for aspartate may be tolerated at only one of the two sites. The examination of the substrate binding constants with mutant enzymes that possessed some activities indicated some changes in the $K_{M.dNTP}$ (Table 1).

There was a decrease in the affinity for dNTP binding by about 10 and 100fold with D378E and D531E. We were unable to determine $K_{M.dNTP}$ for D380E as this enzyme did not display any activity even at high concentrations of substrate dNTP. Furthermore, the binding affinity for template primer ($K_{D.DNA}$) also did not change significantly with alanine or glutamate mutant enzymes, implying no role of catalytic aspartates in the binding of template-primer. The observation that Mn^{2+}-dNTP could be accepted as a substrate at any one of the two mutated positions, with slightly shorter acidic chain, suggest that Mn^{2+} can bind to carboxylate oxygens at positions 378 and 531, and fulfill the function of metal B moiety in Steitz's two metal ion mechanism for polymerases (35). However, mutant enzymes, D380A and D380E did not show any activity with either Mg^{2+} or Mn^{2+} catalyzed reactions implying the absolute need for aspartic acid at this position. Therefore, we conclude that D380 is the ligand for metal A (catalytic metal) and it is involved in the chemistry of bond formation reaction.

The crystal structures of apo (3) and ternary complex of pol III (37) suggest subtle characteristic differences among three catalytic aspartates. A close up of the active site in apo enzyme of *T.acquaticus* pol III is shown in Figure 2A, whereas Figure 2B shows the superposition of apo and ternary complex of *T.acquaticus* pol III. In the apo enzyme, one metal ion is present at the active site even in the absence of template-primer and dNTP. This metal ion (metal A) is 2.6 Å from OD2 atom of D463 and 2.2 Å from OD1 atom of D465. Interestingly, D618 does not interact with this metal. Instead, D618 forms a salt bridge with K616 (between NZ atom of K616 and OD1 atom of D463). An additional metal (metal B) can only be seen in the ternary complex (Figure 2B), which coordinates only with D465 and D463, and the phosphate moiety of incoming dNTP. D616 does not form any coordination with the metals present in the ternary complex crystal structures. It may be pointed out here that D463, D465, D618 and K 616 seen in the crystal structure are equivalent to D378, D380, D531 and K529 of Gka pol E. Therefore, the structural data together with mutant enzyme studies discussed above, suggest that D378 and D380 are stably metal chelated, whereas D531 may have transient coordination with metal ion.

In summary, our results with the catalytic carboxylate triad in *Gka* DNA pol III show that two of the three aspartates, one from the pair in one motif and the other from a distal motif, are involved in the substrate dNTP binding, while the remaining one is involved in the process of phos-

phodiester bond formation.

ACKNOWLEDGEMENTS

This study was supported by a scholarship to C. Sandalli from TUBİTAK.

Other articles in this theme issue include references (38-65).

REFERENCES

1. Arrigo, C. J., Singh, K., and Modak, M. J. DNA polymerase I of *Mycobacterium tuberculosis*: functional role of a conserved aspartate in the hinge joining the M and N helices. *J. biol. chem.* 2002, **277**: 1653-1661.

2. Astatke, M., Grindley, N. D., and Joyce, C. M. Deoxynucleoside triphosphate and pyrophosphate binding sites in the catalytically competent ternary complex for the polymerase reaction catalyzed by DNA polymerase I (Klenow fragment). *J. biol. chem.* 1995, **270**: 1945-1954.

3. Bailey, S., Wing, R. A., and Steitz, T. A. The structure of *T. aquaticus* DNA polymerase III is distinct from eukaryotic replicative DNA polymerases. *Cell.* 2006, **126**: 893-904.

4. Bermek, O., Grindley, N. D., and Joyce, C. M. Distinct roles of the active-site Mg^{2+} ligands, Asp882 and Asp705, of DNA polymerase I (Klenow fragment) during the prechemistry conformational transitions. *J. biol. chem.* 2011, **286**: 3755-3766.

5. Chowdhury, K., Kaushik, N., Pandey, V. N., and Modak, M. J. Elucidation of the role of Arg 110 of murine leukemia virus reverse transcriptase in the catalytic mechanism: biochemical characterization of its mutant enzymes. *Biochem.* 1996, **35**: 16610-16620.

6. Delarue, M., Poch, O., Tordo, N., Moras, D., and Argos, P. An attempt to unify the structure of polymerases. *Prot. Eng.* 1990, **3**: 461-467.

7. Ding, J., Das, K., Hsiou, Y., Sarafianos, S. G., Clark, A. D., Jr., Jacobo-Molina, A., Tantillo, C., Hughes, S. H., and Arnold, E. Structure and functional implications of the polymerase active site region in a complex of HIV-1 RT with a double-stranded DNA template-primer and an antibody Fab fragment at 2.8 A resolution. *J. mol. biol.* 1998, **284**: 1095-1111.

8. Doublie, S., and Ellenberger, T. The mechanism of action of T7 DNA polymerase. *Curr Opin Struct Biol.* 1998, **8**: 704-712.

9. Evans, R. J., Davies, D. R., Bullard, J. M., Christensen, J., Green, L. S., Guiles, J. W., Pata, J. D., Ribble, W. K., Janjic, N., and Jarvis, T. C. Structure of PolC reveals unique DNA binding and fidelity determinants. *Proc nat acad sci USA.* 2008, **105**: 20695-20700.

10. Franklin, M. C., Wang, J., and Steitz, T. A. Structure of the replicating complex of a pol alpha family DNA polymerase. *Cell.* 2001, **105**: 657-667.

11. Gangurde, R., Kaushik, N., Singh, K., and Modak, M. J. A carboxylate triad is essential for the polymerase activity of *Escherichia coli* DNA polymerase I (Klenow fragment). Presence of two functional triads at the catalytic center, *J. biol. chem.* 2000, **275**: 19685-19692.

12. Gangurde, R., and Modak, M. J. Participation of Active-Site Carboxylates of *Escherichia coli* DNA Polymerase I (Klenow Fragment) in the Formation of a Prepolymerase Ternary Complex. *Biochem.* 2002, **41**: 14552-14559.

13. Huang, H., Chopra, R., Verdine, G. L., and Harrison, S. C. Structure of a covalently trapped catalytic complex of HIV-1 reverse transcriptase: implications for drug resistance. *Science.* 1998, **282**: 1669-1675.

14. Ito, J., and Braithwaite, D. K. Yeast mitochondrial DNA polymerase is related to the family: A DNA polymerases. *Nucleic acids res*. 1990, **18**: 6716.

15. Ito, J., and Braithwaite, D. K. Compilation and alignment of DNA polymerase sequences. *Nucleic acids res*. 1991, **19**: 4045-4057.

16. Jacobo-Molina, A., Clark, A. D., Jr., Williams, R. L., Nanni, R. G., Clark, P., Ferris, A. L., Hughes, S. H., and Arnold, E. Crystals of a ternary complex of human immunodeficiency virus type 1 reverse transcriptase with a monoclonal antibody Fab fragment and double-stranded DNA diffract x-rays to 3.5-A resolution. *Proc nat acad sci USA.* 1991, **88**: 10895-10899.

17. Johnson, K. A. Conformational coupling in DNA polymerase fidelity. *Annu rev biochem.* 1993, **62**: 685-713.

18. Joyce, C. M., and Steitz, T. A. Function and structure relationships in DNA polymerases. *Annu. rev. of biochem.* 1994, **63**: 777-822.

19. Kaushik, N., Pandey, V. N., and Modak, M. J. Significance of the O-helix residues of *Escherichia coli* DNA polymerase I in DNA synthesis: dynamics of the dNTP binding pocket, *Biochem.* 1996, **35**: 7256-7266.

20. Kaushik, N., Rege, N., Yadav, P. N., Sarafianos, S. G., Modak, M. J., and Pandey, V. N. Biochemical analysis of catalytically crucial aspartate mutants of human immunodeficiency virus type 1 reverse transcriptase. *Biochem.* 1996, **35**: 11536-11546.

21. Kohlstaedt, L. A., Wang, J., Friedman, J. M., Rice, P. A., and Steitz, T. A. Crystal structure at 3.5 A resolution of HIV-1 reverse transcriptase complexed with an inhibitor. *Science.* 1992, **256**: 1783-1790.

22. Li, Y., Kong, Y., Korolev, S., and Waksman, G. Crystal structures of the Klenow fragment of Thermus aquaticus DNA polymerase I complexed with deoxyribonucleoside triphosphates. *Protein science : a publication of the Protein Society.* 1998, **7**: 1116-1123.

23. Ollis, D. L., Brick, P., Hamlin, R., Xuong, N. G., and Steitz, T. A. Structure of large fragment of *Escherichia coli* DNA polymerase I complexed with dTMP. *Nature.* 1985, **313**: 762-766.

24. Pelletier, H., Sawaya, M. R., Kumar, A., Wilson, S. H., and Kraut, J. Structures of ternary complexes of rat DNA polymerase beta, a DNA template-primer, and ddCTP. *Science.* 1994, **264**: 1891-1903.

25. Polesky, A. H., Steitz, T. A., Grindley, N. D., and Joyce, C. M. Identification of residues critical for the polymerase activity of the Klenow fragment of DNA polymerase I from *Escherichia coli*. *J. biol. chem.* 1990, **265**: 14579-14591.

26. Polesky, A. H., Dahlberg, M. E., Benkovic, S. J., Grindley, N. D., and Joyce, C. M. Side chains involved in catalysis of the polymerase reaction of DNA polymerase I from *Escherichia coli*. *J. biol. chem.* 1992, **267**: 8417-8428.

27. Pritchard, A. E., and McHenry, C. S. Identification of the acidic residues in the active site of DNA polymerase III. *J. mol. biol.* 1999, **285**: 1067-1080.

28. Sandalli, C., Singh, K., Modak, M. J., Ketkar, A., Canakci, S., Demir, I., and Belduz, A. O. A new DNA polymerase I from *Geobacillus caldoxylosilyticus* TK4: cloning, characterization, and mutational analysis of two aromatic residues. *App. microbiol and biotechnol.* 2009, **84**: 105-117.

29. Sanger, F., Nicklen, S., and Coulson, A. R. DNA sequencing with chain-terminating inhibitors. *Proc nat acad sci USA.* 1977, **74**: 5463-5467.

30. Sawaya, M. R., Prasad, R., Wilson, S. H., Kraut, J., and Pelletier, H. Crystal structures of human DNA polymerase beta complexed with gapped and nicked DNA: evidence for an induced fit mechanism. *Biochem.* 1997, **36**: 11205-11215.

31. Singh, K., and Modak, M. J. A unified DNA- and dNTP-binding mode for DNA polymerases. *Trends Biochem Sci.* 1998, **23**: 277-281.

32. Singh, K., and Modak, M. J. Presence of 18-A long hydrogen bond track in the active site of *Escherichia coli* DNA polymerase I (Klenow fragment). Its requirement in the stabilization of enzyme-template-primer complex. *J. biol. chem.* 2003, **278**: 11289-11302.

33. Steitz, T. A., and Steitz, J. A. A general two-metal-ion mechanism for catalytic RNA. *Proc nat acad sci USA.* 1993, **90**: 6498-6502.

34. Steitz, T. A., Smerdon, S. J., Jager, J., and Joyce, C. M. A unified polymerase mechanism for nonhomologous DNA and RNA polymerases. *Science.* 1994, **266**: 2022-2025.

35. Steitz, T. A. DNA polymerases: structural diversity and common mechanisms. *J. biol. chem.* 1999, **274**: 17395-17398.

36. Yin, Y. W., and Steitz, T. A. The structural mechanism of translocation and helicase activity in T7 RNA polymerase. *Cell.* 2004, **116**: 393-404.
37. Wing, R. A., Bailey, S., and Steitz, T. A. Insights into the replisome from the structure of a ternary complex of the DNA polymerase III alpha-subunit, *J. mol. biol.* 2008, **382**: 859-869.
38. Singh, M. P., and Kumar, V., Biodegradation of vegetable and agrowastes by *Pleurotus sapidus*: A noble strategy to produce mushroom with enhanced yield and nutrition. *Cell. Mol. Biol.* 2012, **58** (1): 1-7.
39. Pandey, V. K., Singh, M.P., Srivastava, A. K., Vishwakarma S. K., and Takshak, S., Biodegradation of sugarcane bagasse by white rot fungus *Pleurotus citrinopileatus. Cell. Mol. Biol.* 2012, **58** (1): 8-14.
40. Ruhal, A., Rana, J. S., Kumar S., and Kumar, A., Immobilization of malate dehydrogenase on carbon nanotubes for development of malate biosensor. *Cell. Mol. Biol.* 2012, **58** (1): 15-20.
41. Vishwakarma, S. K., Singh, M. P., Srivastava A.K. and Pandey, V. K., Azo dye (direct blue) decolorization by immobilized extracellular enzymes of *Pleurotus* species. *Cell. Mol. Biol.* 2012, **58** (1): 21-25.
42. Dash, S. K., Sharma, M., Khare, S. and Kumar, A., *rmpM* gene as a genetic marker for human bacterial meningitis. *Cell. Mol. Biol.* 2012, **58** (1): 26-30.
43. Bertoletti, F., Crespan, E. and Maga, G., Tyrosine kinases as essential cellular cofactors and potential therapeutic targets for human immunodeficiency virus infection. *Cell. Mol. Biol.* 2012, **58** (1): 31-43.
44. Kaushal, A., Kumar, D., Khare, S. and Kumar, A., *speB* gene as a specific genetic marker for early detection of rheumatic heart disease in human. *Cell. Mol. Biol.* 2012, **58** (1): 50-54.
45. Datta, J. and Lal, N., Application of molecular markers for genetic discrimination of *fusarium* wilt pathogen races affecting chickpea and pigeonpea in major regions of India. *Cell. Mol. Biol.* 2012, **58** (1): 55-65.
46. Siddiqi, N. J., Alhomida, A. S., Khan, A. H. and Onga, W.Y., Study on the distribution of different carnitine fractions in various tissues of bovine eye. *Cell. Mol. Biol.* 2012, **58** (1): 66-70.
47. Ong, Y. T., Kirby, K. A., Hachiya, A., Chiang, L. A., Marchand, B., Yoshimura, K., Murakami, T., Singh, K., Matsushita, S. and Sarafianos, S. G., Preparation of biologically active single-chain variable antibody fragments that target the HIV-1 GP120 v3 loop. *Cell. Mol. Biol.* 2012, **58** (1): 71-79.
48. Singh, J., Gautam, S. and Bhushan Pant, A., Effect of UV-B radiation on UV absorbing compounds and pigments of moss and lichen of Schirmacher Oasis region, East Antarctica. *Cell. Mol. Biol.* 2012, **58** (1): 80-84.
49. Singh, V. P., Srivastava, P. K., and Prasad, S. M., Impact of low and high UV-B radiation on the rates of growth and nitrogen metabolism in two cyanobacterial strains under copper toxicity. *Cell. Mol. Biol.* 2012, **58** (1): 85-95.
50. Datta, J. and Lal, N., Temporal and spatial changes in phenolic compounds in response *Fusarium* wilt in chickpea and pigeonpea. *Cell. Mol. Biol.* 2012, **58** (1): 96-102.
51. Sharma, R. K., JAISWAL, S. K., Siddiqi, N. J., and Sharma, B., Effect of carbofuran on some biochemical indices of human erythrocytes *in vitro. Cell. Mol. Biol.* 2012, **58** (1): 103-109.
52. Singh, A. K., Singh, S. and Singh, M. P., Bioethics A new frontier of biological Science. *Cell. Mol. Biol.* 2012, **58** (1): 110-114.
53. Adedeji, A. O., Singh, K. and Sarafianos, S. G., Structural and biochemical basis for the difference in the helicase activity of two different constructs of SARS-CoV helicase. *Cell. Mol. Biol.* 2012, **58** (1): 115-121.
54. Singh, S., Choudhuri, G., Kumar, R. and Agarwal, S., Association of 5, 10-methylenetetrahydrofolate reductase C677T polymorphism in susceptibility to tropical chronic pancreatitis in North Indian population. *Cell. Mol. Biol.* 2012, **58** (1): 122-127.
55. Sharma, R. K., Rai, K. D. and Sharma, B., *In* vitro carbofuran induced micronucleus formation in human blood lymphocytes. *Cell. Mol. Biol.* 2012, **58** (1): 128-133.
56. Naraian, R., Ram, S., Kaistha S. D. and Srivastava J., Occurrence of plasmid linked multiple drug resistance in bacterial isolates of tannery effluent. *Cell. Mol. Biol.* 2012, **58** (1): 134-141.
57. Pandey, A. K., Mishra, A. K., And Mishra, A., Antifungal and antioxidative potential of oil and extracts, respectively derived from leaves of Indian spice plant *Cinnamomum tamala. Cell. Mol. Biol.* 2012, **58** (1): 142-147.
58. Mishra, N., and Rizvi, S. I., Quercetin modulates na/k atpase and sodium hydrogen exchanger in type 2 diabetic erythrocytes. *Cell. Mol. Biol.* 2012, **58** (1): 148-152.
59. Kumar, A., Sharma, B. and Pandey, R. S., Assessment of stress in effect to pyrethroid insecticides, λ-cyhalothrin and cypermethrin in a freshwater fish, *Channa punctatus* (Bloch). *Cell. Mol. Biol.* 2012, **58** (1): 153-159.
60. Srivastava N., Sharma, R. K., Singh, N. and Sharma, B., Acetylcholinesterase from human erythrocytes membrane: a screen for evaluating the activity of some traditional plant extracts. *Cell. Mol. Biol.* 2012, **58** (1): 160-169.
61. Singh, M.P., Pandey, A. K., Vishwakarma S. K., Srivastava, A. K. and Pandey, V. K., Extracellular Xylanase Production by *Pleurotus* species on Lignocellulosic Wastes under *in vivo* Condition using Novel Pretreatment. *Cell. Mol. Biol.* 2012, **58** (1): 170-173.
62. Kumar, S., Sharma, U. K., Sharma, A. K., Pandey, A. K., Protective efficacy of *Solanum xanthocarpum* root extracts against free radical damage: phytochemical analysis and antioxidant effect. *Cell. Mol. Biol.* 2012, **58** (1): 174-181.
63. Shukla, A., Singh, A., Singh, A., Pathak, L.P., Shrivastava, N., Tripathi, P. K., Singh, K. and Singh, M.P., Inhibition of *P. falciparum* pfATP6 by curcumin and its derivatives: A bioinformatic Study. *Cell. Mol. Biol.* 2012, **58** (1): 182-186.
64. Michailidis, E., Singh, K., Ryan, E. M., Hachiya, A., Ong, Y. T., Kirby, K. A., Marchand, B., Kodama, E. N., Mitsuya, H., Parniak, M.A. and Sarafianos, S.G., Effect of translocation defective reverse transcriptase inhibitors on the activity of n348i, a connection subdomain drug resistant HIV-1 reverse transcriptase mutant. *Cell. Mol. Biol.* 2012, **58** (1): 187-195.
65. Parveen, A., Rizvi, S. H. M., Gupta, A., Singh, R., Ahmad, I., Mahdi, F., and Mahdi, A. A., NMR-based metabonomics study of sub-acute hepatotoxicity induced by silica nanoparticles in rats after intranasal exposure. *Cell. Mol. Biol.* 2012, **58** (1): 196-203.